

Proceedings of the International Conference on Oxide Materials for Electronic Engineering, May 29–June 2, 2017, Lviv

Optical Properties of GGG Epitaxial Films Grown from PbO–B₂O₃–V₂O₅ Flux

I.I. SYVOROTKA^{a,b,*}, D.YU. SUGAK^{a,b}, A.P. LUCHECHKO^c, YA.A. ZHYDACHEVSKYY^{b,d}
AND S.B. UBIZSKI^b

^aScientific Research Company “Carat”, Lviv, Ukraine

^bLviv Polytechnic National University, Lviv, Ukraine

^cIvan Franko National University of Lviv, Lviv, Ukraine

^dInstitute of Physics, Polish Academy of Sciences, Warsaw, Poland

The paper reports a growth of the high-quality Gd₃Ga₅O₁₂ (GGG) homoepitaxial films by the liquid phase epitaxy technique using the PbO–B₂O₃ and PbO–B₂O₃–V₂O₅ fluxes. The influence of the flux composition containing V₂O₅ as well as the growth temperature is discussed basing on the optical absorption and the electron probe micro analysis results.

DOI: [10.12693/APhysPolA.133.954](https://doi.org/10.12693/APhysPolA.133.954)

PACS/topics: 81.15.Lm, 78.66.Nk

1. Introduction

Garnet crystals are known to be used as materials for solid-state lasers including the lasers with passive Q-switching in the range of 1–1.6 μm. Single crystalline films grown by the liquid phase epitaxy (LPE) have some advantages in comparison with bulk crystals such as homogeneity, structural perfection, optical transparency, etc.

The present work is devoted to growth of the high-quality gadolinium gallium garnet Gd₃Ga₅O₁₂ (GGG) homoepitaxial films. An influence of the flux composition containing V₂O₅ on optical properties of the GGG epitaxial films is discussed.

2. Experimental

Single crystalline films of GGG were grown by the standard LPE method from a supersaturated melt on the base of PbO–B₂O₃ and PbO–B₂O₃–V₂O₅ fluxes. All technological experiments were carried out on air using the five-heating-zone LPE furnace “Garnet-3” (LPAI, France). To keep the crucible temperature on given level in the range of 600–1200 °C with high precision (±0.1 °C) the furnace was self-modernized by adding an adaptive double-loop feedback temperature regulation system.

To calculate a charge composition for growth GGG films the following molar ratios (the Blank–Nielsen coefficients) were used:

$$R_1 = \frac{\text{Ga}_2\text{O}_3}{\text{Gd}_2\text{O}_3},$$

$$R_3 = \frac{\text{PbO}}{\text{B}_2\text{O}_3},$$

$$R_4 = \frac{\text{Gd}_2\text{O}_3 + \text{Ga}_2\text{O}_3}{\text{Gd}_2\text{O}_3 + \text{Ga}_2\text{O}_3 + \text{PbO} + \text{B}_2\text{O}_3 + \text{V}_2\text{O}_5} \times 100\%,$$

$$R_5 = \frac{\text{PbO}}{\text{V}_2\text{O}_5}. \quad (1)$$

Molar ratios were chosen in such a way that would provide crystallization of garnet phase. For determine these value the data from [1, 2] was analyzed. The part of Gd₂O₃–Ga₂O₃–(PbO–n × B₂O₃) composition triangle based on analyzed data and chosen value for growth GGG films is present in Fig. 1. The melts compositions and molar ratios of the melts are given in Table I.

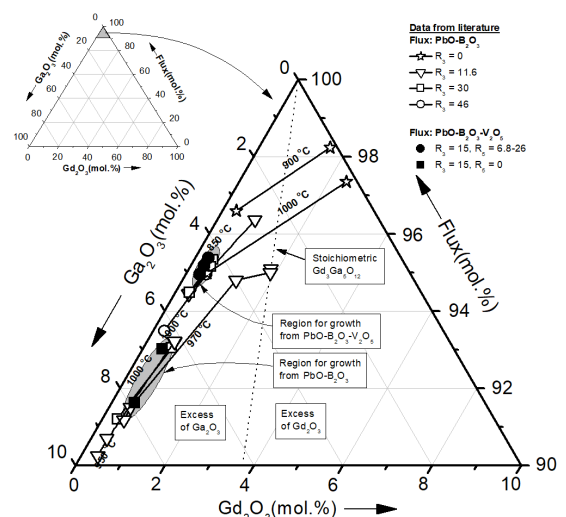


Fig. 1. Part of the Gd₂O₃–Ga₂O₃–(PbO–n × B₂O₃) composition triangle.

*corresponding author; e-mail: syvorotka.jr@yahoo.com

TABLE I

Molar content of the melts

Flux	PbO		B ₂ O ₃		V ₂ O ₅		Gd ₂ O ₃		Ga ₂ O ₃		Molar coefficient			
	[g]	[mol.%]	[g]	[mol.%]	[g]	[mol.%]	[g]	[mol.%]	[g]	[mol.%]	R ₁	R ₃	R ₄	R ₅
3G-A0	915.794	87.204	19.053	5.816	0	0	7.444	0.436	57.726	6.545	15.0	15.0	6.98	0
3G-A0	915.794	87.25	19.053	5.82	0	0	7.000	0.405	57.200	6.500	16.0	15.0	6.98	0
3G-A1	930.850	85.974	19.050	5.642	0	0	9.235	0.525	71.460	7.859	15.0	15.0	8.38	0
GV	905.615	85.950	18.716	5.690	28.376	3.300	5.400	0.315	41.892	4.734	15.0	15.0	5.05	26.0
2GV	905.615	82.125	18.716	5.441	68.376	7.609	5.400	0.301	41.892	4.523	15.0	15.0	4.82	10.8
3GV	905.615	78.625	18.716	5.209	108.376	11.546	5.400	0.288	41.892	4.330	15.0	15.0	4.62	6.8

Experiments on the film growth were carried out in two steps. The first one applied for obtaining GGG films from PbO–B₂O₃. The second one — with addition of V₂O₅ into the melt.

The garnet-forming components (Gd₂O₃ and Ga₂O₃) weighed in appropriate ratio were pre-melted in platinum crucible height together with the flux components (PbO, B₂O₃ and V₂O₅). To dissolve the garnet-forming components completely and to homogenize the melt, a crucible content was maintained in growth furnace during few hours at temperature to be 100–150 °C over the saturation temperature with respect to garnet phase. After reliable homogenization, the melt temperature was slowly decreased till the growth temperature that was 5–60 °C lower than the saturation point, and a prepared substrate held horizontally was dipped into the fluxed melt and held there for appropriate time depending on the film thickness needed. As substrates the (111)-oriented epitaxial grade single crystalline GGG plates (with the lattice parameter 12.382 Å and thickness of 460–490 μm) were used. During the growth process the substrate was reversely rotated with the rate of 60 rpm.

After withdrawing from solution the rotation rate was increased up to 200–400 rpm to remove any residual flux from the layer surface. A thickness of the grown films was determined by the weighting method taking into account the computed film density.

The growth temperature was in the range of 880–1010 °C. The films with thickness of 4–60 μm were grown at growth rate changing from 0.1 to 1.0 μm/min. The films grown from 3G and GV fluxes were colorless and transparent, but films grown from 2GV and 3GV fluxes had purple color. The temperature dependences of the growth rate for the GGG films grown from different fluxes are shown in Fig. 2.

The substrate and film lattice parameters were determined by $\theta - 2\theta$ standard X-ray diffraction (XRD) method using a DRON-3 (Burevestnik, Russia) diffractometer with an X-ray source emitting the Cu $K_{\alpha 1}$ line at $\lambda = 1.540562$ Å. As a reference point the (888) diffraction peak with $2\theta = 119.1^\circ$ was used for measurement of the (111)-oriented structures. The lattice parameter a_f of the strain-free epitaxial film can be obtained using the Poisson coefficient ν :

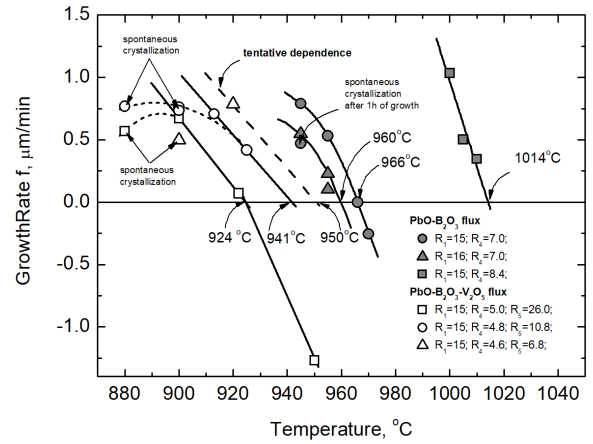


Fig. 2. Temperature dependences of the growth rate for the GGG films grown from different fluxes.

$$a_f = (a_e - a_s) \frac{1 - \nu}{1 + \nu} + a_s, \quad (2)$$

where a_s is the lattice parameter of the substrate and a_e is the lattice parameter of the epitaxial film.

The content of Pb, Pt, and V ions in the grown films was analysed by the electron probe micro analysis (EPMA). Optical absorption spectra of the grown films were obtained from the transmission spectra measured by a Shimadzu UV-3600 (Japan) spectrophotometer at room temperature in the spectral range 200–1500 nm.

Some samples were annealed in vacuum or air at 900 °C. The annealing was carried out in a Nabertherm Supertherm LHT 04/17 furnace.

3. Results and discussion

For investigation of optical properties, the series of GGG epitaxial films grown from fluxes with different concentration of V₂O₅ were chosen. Main growth parameters of the studied films are present in Table II.

As follows from microanalysis results, all the studied films contain Pt and Pb ions. Films grown from fluxes based on PbO–B₂O₃–V₂O₅ also contain vanadium, but in very low concentrations. Besides, the films grown from the fluxes with the concentration of V₂O₅ of 7.6 and 11.5 mol.% (fluxes 2GV and 3GV, respectively) contain

significantly more lead ions than films grown from fluxes with a low concentration of V_2O_5 (3.3 mol.%) or without V_2O_5 . The highest concentration of Pb ions (0.332 at.%) has been observed in the film 2GV-1, which was grown at the lowest growth temperature (880 °C). The Pb and Pt

ions concentrations as a function of the growth temperature for the GGG films grown from $PbO-B_2O_3-V_2O_5$ fluxes are shown in Fig. 3. As it is seen from the figure, the concentrations of Pb and Pt ions increase with decrease of growth temperature for all the fluxes.

TABLE II

Main growth parameters of the studied films

ID	Flux	Flux composition [mol.%]				Growth parameters		Films parameters			Chemical composition of films (EPMA) [at.%]		
		PbO	B ₂ O ₃	V ₂ O ₅	T _s , °C	f, μm/min	T _g , °C	h, μm	a, Å	Δ a, 10 ⁻³ Å	Pt	Pb	V
3G-3	PbO-B ₂ O ₃	87.25	5.82	0	966	0.790	945	15.81	12.3754	-5.52	0.032	0.022	-
3G-9		85.97	5.64	0	1014	0.346	1010	14.02	12.3749	-6.06	0.024	0.008	-
GV-3	PbO-B ₂ O ₃ -V ₂ O ₅	85.95	5.69	3.30	924	0.570	880	34.19	12.3753	-6.0	0.082	0.030	0.038
2GV-1						0.768	880	46.08	12.3773	-4.0	0.068	0.332	0.024
2GV-2						0.760	900	11.44	12.3752	-6.1	0.040	0.148	0.020
2GV-3						0.708	913	24.78	12.3747	-6.6	0.030	0.068	0.015
3GV-1						0.785	920	47.11	12.3781	-3.2	0.006	0.064	0.012
3GV-2						0.499	900	29.91	12.3759	-5.4	0.016	0.138	0.014
			78.63	5.21	11.55	950							

TABLE III

Observed absorption bands and corresponding optical transitions in the studied GGG epitaxial films

Wavelength [nm]	Energy [cm ⁻¹]	Transition description	Ref.
254	39370	A	[4, 5]
273	36630		
306	32680		
312	32050		
280	35700	B	[3, 6, 7]
322	31000	C	[3, 6, 7]
550	18180	D	[3, 6, 7]

A — Intra-center transitions of f -electrons in Gd^{3+} (transition from ground $^8S_{7/2}$ state to split by crystal field multiplets 6P , 6I and 6D terms), B — Electron transition $^1S_0 \rightarrow ^3P_1$ of $Pb^{2+}(6s^2)$, C — Charge transfer from the oxygen band to Pb^{4+} $O^{2-} + Pb^{4+} + h\nu \rightarrow Pb^{3+} + O^-$, D — Intervalence transition $Pb^{2+} + Pb^{4+} + h\nu \rightarrow Pb^{3+} + Pb^{3+}$

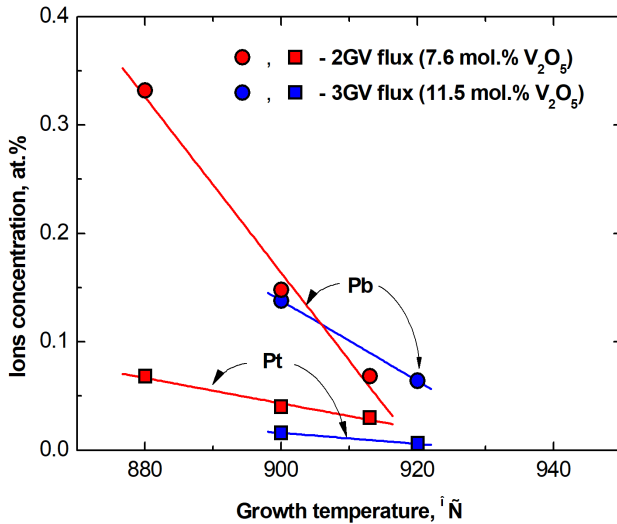


Fig. 3. The Pb and Pt ions concentration dependences from the growth temperature for the GGG films grown from $PbO-B_2O_3-V_2O_5$ fluxes.

The main absorption bands and the corresponding transitions observed in the GGG structures grown from the PbO -based flux are present in Table III. Optical absorption spectra of the investigated GGG films grown from $PbO-B_2O_3$ and $PbO-B_2O_3-V_2O_5$ fluxes are shown in Fig. 4. As can be seen from the obtained spectra the absorption band at 280 nm, which corresponds to electron transition $(6s^2)^1S_0 \rightarrow ^3P_1$ of Pb^{2+} ions [3], is observed in all films grown from both fluxes. The additional absorption bands were observed in films grown from the $PbO-B_2O_3-V_2O_5$ flux (Fig. 4b,c). The first one with maximum at 322 nm corresponds to charge transfer from the oxygen to Pb^{4+} ($O^{2-} + Pb^{4+} + h\nu \rightarrow Pb^{3+} + O^-$)

and the second one with maximum at 550 nm is due to intervalence pairwise transitions in Pb^{2+} and Pb^{4+} ions ($Pb^{2+} + Pb^{4+} + h\nu \rightarrow Pb^{3+} + Pb^{3+}$) [3]. At the same time any absorption peaks, which can correspond to V^{3+} or V^{4+} ions, were not detected.

The absorption spectra of GGG films grown at the same temperature, but from fluxes containing different concentrations of V_2O_5 , are present in Fig. 4c. It is seen that with increase of V_2O_5 content in the flux (decreasing the molar ratio R_5) the increase of intensity of the absorption bands at 280 nm and 322 nm (related to Pb^{2+} and Pb^{4+} ions), as well as the absorption with maximum at 550 nm (related to intervalence pairwise transitions of Pb) is observed. Figure 4b shows the optical absorption spectra of the films grown from the flux with a constant concentration of V_2O_5 at different temperatures. With

decrease of growth temperature, the intensities of the absorption bands at 280, 322, and 550 nm are increasing. In such a way analyzing the optical absorption spectra of the grown films and taking into account the data of

microanalysis, we can conclude that vanadium oxide in the fluxes behaves as a flux component and stimulates the occurrence of Pb ions in the films as well as leads to formation of the Pb^{2+} - Pb^{4+} pairs.

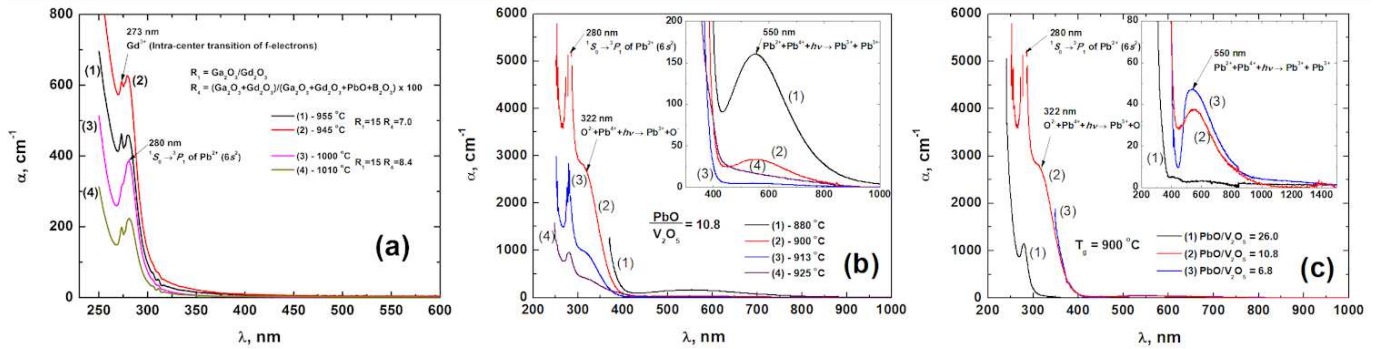


Fig. 4. The optical absorption spectra of the GGG films grown from the $\text{PbO-B}_2\text{O}_3$ (a) and the $\text{PbO-B}_2\text{O}_3\text{-V}_2\text{O}_5$ (b, c) fluxes at different temperatures (b) and different V_2O_5 content (c).

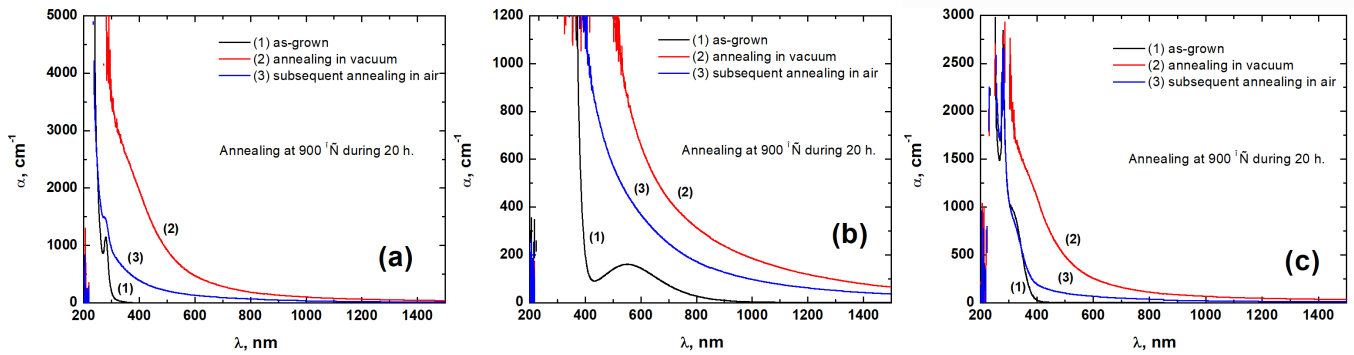


Fig. 5. Optical absorption spectra of the studied GGG films (as-grown and annealed) grown from $\text{PbO-B}_2\text{O}_3\text{-V}_2\text{O}_5$ fluxes. (a) Film GV-2 grown at 900°C ($R_5 = 6.8$); (b) film 2GV-1 grown at 880°C ($R_5 = 10.8$); (c) film 2GV-3 grown at 913°C ($R_5 = 10.8$).

An influence of heat treatment in reducing or oxidizing atmosphere on the optical properties of the GGG films was also investigated. For this purpose, the annealing in vacuum and in air at temperature 900°C during 20 h was carried out. The optical absorption spectra of the films grown at different temperatures from fluxes with different concentrations of V_2O_5 (molar ratios $R_5 = 6.8, 10.8$) after annealing in vacuum and subsequent annealing in air are shown in Fig. 5. It was found that annealing in vacuum leads to a significant increase of absorption in the whole investigated spectral range for all the samples. It should be noted that the subsequent annealing in air does not lead to reversible changes.

4. Conclusions

A series of GGG films were grown on the (111)-oriented GGG substrates using the $\text{PbO-B}_2\text{O}_3$ and $\text{PbO-B}_2\text{O}_3\text{-V}_2\text{O}_5$ fluxes. The absorption band at 280 nm related to Pb^{2+} ions was observed for all the grown films. The additional absorption bands at 322 nm (caused by Pb^{4+} ions) and at 550 nm (caused by Pb^{2+} and Pb^{4+} ions) were

observed for the films grown from the $\text{PbO-B}_2\text{O}_3\text{-V}_2\text{O}_5$ flux. An increase of V_2O_5 content in the flux or decrease of the growth temperature leads to increase of intensity of the absorption bands at 280, 322, and 550 nm.

Basing on data of microanalysis and optical absorption spectra it was concluded that the V_2O_5 in the fluxes behaves as a flux component. Moreover, the addition of V_2O_5 into the melt stimulates incorporation of Pb ions into the GGG films and leads to formation of the Pb^{2+} - Pb^{4+} pairs. At the same time any absorption peaks, which can correspond to V^{3+} or V^{4+} ions, were not detected.

An annealing of the GGG films in vacuum leads to significant increase of absorption in the whole investigated spectral range. The subsequent annealing of the films in air does not lead to reversible changes.

Acknowledgments

This research was supported by the Ministry of Education and Science of Ukraine (project DB/EMSh, 0116U004134) and by the Polish National Science Center (project 2015/17/B/ST5/01658).

References

- [1] E.A. Giess, M.M. Faktor, R. Ghez, C.F. Guerci, *J. Cryst. Growth* **56**, 576 (1982).
- [2] G.A. Bufetova, M.Yu. Gusev, I.A. Ivanov, N.S. Neustroev, D.A. Nikolaev, V.F. Seregin, V.B. Tsvetkov, I.A. Shcherbakov, *Phys. Wave Phenom.* **17**, 77 (2009).
- [3] G.B. Scott, J.L. Page, *J. Appl. Phys.* **48**, 1342 (1977).
- [4] A. Matkovskii, P. Potera, D. Sugak, L. Grigorjeva, D. Millers, V. Pankratov, A. Suchocki, *Cryst. Res. Technol.* **39**, 788 (2004).
- [5] V.V. Randoshkin, N.V. Vasil'eva, V.G. Plotnichenko, Yu.N. Pyrkov, S.V. Lavrishchev, M.A. Ivanov, A.A. Kiryukhin, A.M. Saletskii, N.N. Sysoev, *Phys. Solid State* **46**, 1030 (2004).
- [6] V.V. Randoshkin, N.V. Vasil'eva, A.V. Vasil'ev, V.G. Plotnichenko, S.V. Lavrishchev, A.M. Saletskii, K.V. Stashun, N.N. Sysoev, A.N. Churkin, *Phys. Solid State* **43**, 1659 (2001).
- [7] N.V. Vasil'eva, V.V. Randoshkin, V.G. Plotnichenko, Yu.N. Pyrkov, V.V. Voronov, A.M. Galstyan, N.N. Sysoev, *Inorg. Mater.* **44**, 76 (2008).